PERFORMANCE OF A WIDE ANGLE AND WIDE BAND NULLING METHOD FOR PHASED ARRAYS

Khalil H. Sayidmarie and Jafar R. Mohammed[*]

Department of Communication Engineering, College of Electronic Engineering, University of Mosul, Mosul-41001, Iraq

Abstract—In most practical applications of the phased array antennas, the generated nulls toward the interfering signals should have enough depth and width to accommodate fluctuations in frequency and direction of the interferer. Due to these fluctuations, the nulls can be easily deviated from its desired angular locations in the traditional adaptive nulling arrays since the nulls are very sharp and sensitive. An innovative technique for wide nulling arrays has been recently presented. The wide nulls can be introduced by setting properly the excitation coefficients of the two edge elements of the antenna array. In this paper, the effect of frequency fluctuation on the nulling performance is investigated. By generating wide and deep nulls toward and around the interference directions, the proposed method provides robustness against frequency fluctuation. Simulation results in realistic situations with frequency fluctuation are presented to illustrate the performance of the proposed technique. Comparisons with the standard fully adaptive nulling array are shown.

1. INTRODUCTION

In standard adaptive arrays, the nulls are generally steered toward the interfering signals by controlling the excitation coefficients of all or most of the array elements. However, the resulting nulls are often sharp and very sensitive to many parameters such as; local scattering, direction-of-arrival (DOA) errors of the interfering signals, imperfectly calibrated arrays, mutual coupling effects between array elements, wave-front distortion, spreading of interfering sources, and distorted antenna shape. Since the angular locations of these nulls are very sensitive to the array imperfections, there is a great need to place wide nulls towards unwanted directional interferences.

* Corresponding author: Jafar Ramadhan Mohammed (jafarram@yahoo.com).

Wide nulls are formed in conventional adaptive arrays by placing multiple adjacent nulls in the radiation pattern [1, 2] or by using stochastically optimization approaches to synthesize an antenna pattern having wide nulls at specific directions by imposing some constraints on the adaptive weights [3–6]. Optimization techniques like enhanced particle swarm [7], and sequential quadratic programming [8] algorithms have been used for the synthesis of wide nulls. Alternatively, instead of creating an adaptive wide null in the direction of the interfering signal, it is sometimes more convenient to design an array with decreased sidelobe levels. An interesting example is the use of two additional elements with iterative Fourier transform method to specifically design a phased array with ultra-low sidelobes [9]. However, null forming and sidelobe suppression in these aforementioned approaches require full control of all excitation coefficients (where control could be in any of the following forms: amplitude-and-phase, phase-only, or by amplitude-only) of the array elements. Full control could be prohibitively expensive in many applications and may raise reliability problems when the number of array elements is large. A less costly and complex system is desirable where only a few elements are arranged to be controllable, e.g., adaptive sidelobe canceller (SLC) [10, 11] and partially adaptive arrays [12–14]. The adaptive SLC includes one or more relatively low gain auxiliary element(s) interconnected with the main antenna elements by an adaptive control which combines the signals received by the auxiliary and main antennas to cause partial or complete cancellation of the interfering signals. In this technique, one adaptive control system is required for each interfering signal. However, in many wireless communication systems the direction-of-arrival of the interfering signals may vary with time or may not be known exactly, so each sidelobe canceller must in general change the excitation coefficients of the array elements to track its own interferer signal. In such a case, each sidelobe canceller changes the whole radiation pattern including repositioning of nulls, causing all the other sidelobe cancelling systems to readjust not only in response to their own moving interfering signals, but also to the changing sidelobe structure of the overall radiation pattern. Therefore, these types of adaptive sidelobe cancellers are very complex, and their implementation for more than few interfering signals may be both impractical and prohibitively expensive.

In [15], a technique for obtaining simultaneously wide-angular nulling in the sum and difference patterns of a monopulse array antenna that utilizes two additional elements, each placed at a distance equal to $\lambda/4$ from array side, was introduced, which generated wide nulls

by reusing two of the existing elements of the array while maintaining the same performance for interference suppression. In this paper, we investigate the effect of frequency fluctuation on the generated nulls. By generating wide and deep nulls toward and around the interference directions, the proposed method provides robustness against frequency fluctuation. A wide null at prescribed direction can be introduced by subtracting the weighted pattern of the two edge elements from that of the original N-element uniform array.

2. THE TECHNIQUE

In this section, an ideal situation without frequency fluctuation is assumed, and the antenna is designed at configured frequency f_o. Consider an array is placed along the x-axis, and has N isotropic radiating elements separated by equal intervals of $d = \lambda_o/2$. For simplicity of practical implementation, assume a uniform array of equal weights. The corresponding symmetric array factor will be [16]:

$$AF(\theta) = \frac{\sin\left[\frac{N}{2}kd\sin(\theta)\right]}{\sin\left[\frac{1}{2}kd\sin(\theta)\right]} \tag{1}$$

where $k = \frac{2\pi}{\lambda_o}$ is the wave number and θ is the observation angle from normal to array axis. From (1), the maxima of the sidelobes occur at angles $\theta_{\max}$ [16]

$$\theta_{\max} = \sin^{-1}\left[\frac{\lambda_o}{2\pi d}\left[\pm\frac{2s+1}{N}\pi\right]\right], \quad s = 1, 2, 3, \ldots \tag{2}$$

where $s = 1$ corresponds to the maximum of the first sidelobe. At these angles, the magnitudes of the sth sidelobe can be calculated from (1) as:

$$|AF(\theta_{\max})| = \left|\frac{1}{\sin\left[\frac{\pi}{2}\frac{2s+1}{N}\right]}\right| \tag{3}$$

Let the amplitude excitation of the two side elements be A, and let the phase of their excitation be $-P$, and P. Let a subscript "$-$" denotes the edge element at left and at position $-\frac{N-1}{2}d$ and let a subscript "$+$" denotes the edge element at right and at position $+\frac{N-1}{2}d$. In the far-field region, the cancellation pattern (CP) of these two edge elements at direction $\theta_{\max}$ will be:

$$CP(\theta_{\max}) = Ae^{j\left[\frac{\pi}{2}(N-1)\left(\frac{2s+1}{N}\right)+P\right]} + Ae^{-j\left[\frac{\pi}{2}(N-1)\left(\frac{2s+1}{N}\right)+P\right]}$$

$$= 2A\cos\left[\frac{\pi}{2}(N-1)\left(\frac{2s+1}{N}\right) + P\right] \tag{4}$$

The technique is to set the phase P so that the lobes of the cancellation pattern, due to the two edge elements, are matched in width to the sidelobes of the original array. Then to scale the amplitude of the cancellation pattern by a factor A so that it is equal in magnitude to and in antiphase with the original array pattern at the desired null locations $\theta_{\max}$. The technique is explained as follows. First, in order to obtain wide nulls centered at $\theta_{\max}$, the side lobe maxima, given by Equation (3), should be equal to the maxima of the cancellation pattern which is given by Equation (4), i.e.,

$$CP(\theta_{\max}) = -AF(\theta_{\max}) \tag{5}$$

Next, the scale factor A, and phase shift P of the two edge elements are chosen according to:

$$A = \frac{|CP(\theta_{\max})|}{2} = \frac{|Af(\theta_{\max})|}{2} \tag{6}$$

$$P = -\left[\pi + \frac{\pi}{2}(N-1)\left(\frac{2s+1}{N}\right)\right] \tag{7}$$

so that the main lobe of the cancellation pattern is made coincident with the sidelobe peak of the original N-element uniform array at $\theta_{\max}$. Finally, knowing A and P, the excitations of the two edge elements can be determined. By such way the edge-elements would produce a resulting pattern with wide nulls centered at $\theta_{\max}$. The required excitation (amplitude w and phase $\emptyset$) of the two edge elements which are located at positions $-\frac{N-1}{2}d$ and $+\frac{N-1}{2}d$ can be written as the sum of the original uniform excitation and the readjusted one as:

$$\left|w\left(-\frac{N-1}{2}d\right)\right| = \left|w\left(+\frac{N-1}{2}d\right)\right| = \sqrt{\{(1+A\cos(p))^2 + A^2\sin^2(p)\}} \tag{8}$$

and

$$\emptyset\left(-\frac{N-1}{2}d\right) = -\emptyset\left(+\frac{N-1}{2}d\right) = \tan^{-1}\left\{\frac{A\sin(p)}{1+A\cos(p)}\right\} \tag{9}$$

Here, the wide null is placed in an array pattern by subtracting a cancellation pattern from the original pattern of the uniform array under constraint that the magnitude of the cancellation pattern is equal to that of the original pattern at the desired null locations.

2.1. The Effect of Frequency Fluctuation on Null Position

In this subsection, a realistic situation is investigated where there is fluctuation in the frequency of operation, or the system works on a band of frequencies. It is assumed that the element positions can be

accurately fixed at the design frequency f_o, and element separation is equal to $d = \lambda_o/2$, where λ_o is the free-space wavelength at the design frequency. In this case, the array factor of uniformly excited equally spaced linear array can be found from (1) as:

$$AF(f, \theta) = \frac{\sin\left[\frac{Nf}{2f_o}\pi\sin(\theta)\right]}{\sin\left[\frac{1}{2}\frac{f}{f_o}\pi\sin(\theta)\right]} \qquad (10)$$

where f is instantaneous frequency, and f/f_o is fluctuation or deviation ratio. From (10), the angle of the nth null θ_n as a function of frequency can be written as:

$$\theta_n(f) = \sin^{-1}\left[\frac{f_o}{f}\left(\pm\frac{2n}{N}\right)\right] \qquad (11)$$

A sample array of $N = 10$ elements working at frequency f, and designed at $f_o = 3\,\text{GHz}$, is investigated here. Fig. 1(a) shows the radiation patterns of the uniform array, plotted for frequency values higher than the design value $f_o = 3\,\text{GHz}$. It can be seen that the angular location of the first null, $(n = 1)$, in the uniform pattern is $11.54°$, whereas this null will be shifted to $9.871°$ when f is changed from $3\,\text{GHz}$ to $5\,\text{GHz}$. The figure shows that, as the frequency departs from the design value $f_o = 3\,\text{GHz}$, the nulls move toward main beam resulting in increased magnitude at the original directions of the nulls. Fig. 1(b) shows the radiation patterns of the same array, plotted for frequency values lower than the design value. It can be seen that the angular location of the first null will be shifted from $11.54°$ to $13.8°$ when f is changed from $3\,\text{GHz}$ to $2.5\,\text{GHz}$ whereas the forth null, $n = 4$, will be shifted from $53.33°$ to $74.0°$ when f is changed from $3\,\text{GHz}$ to $2.5\,\text{GHz}$. The figure shows that, as the frequency becomes lower than the design value $f_o = 3\,\text{GHz}$, the nulls move far away from the main beam resulting in increased magnitude at the original directions of the nulls. Generally, it is noticed that the nulls are very sensitive to frequency changes. The sensitivity of the null angle θ_n to frequency can be found from Equation (11) as:

$$\frac{d\theta_n}{df} = \frac{1}{\sqrt{1 - \left(\frac{2nf_0}{Nf}\right)^2}} \qquad (12)$$

The above relation shows that farther nulls (larger values of n) have higher sensitivity, and the sensitivity is a nonlinear function of the frequency deviation. This nonlinearity can be obviously noticed by comparing Figs. 1(a) and 1(b), where a $0.5\,\text{GHz}$ changes in frequency produces different shifts in the null positions. It has been found that a
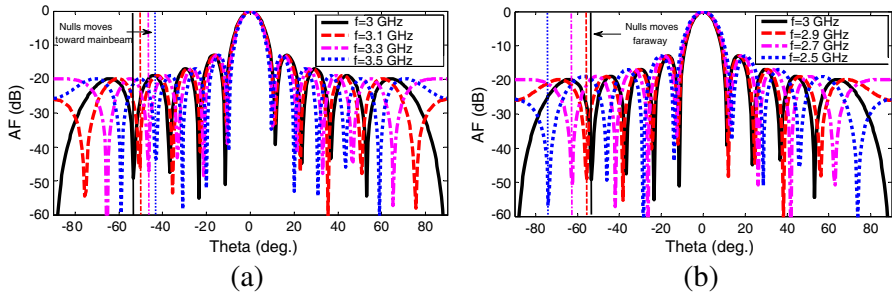
Figure 1. The effect of the frequency changes on the null positions in uniformly excited equally spaced linear array of $N = 10$ elements, design frequency $f_o = 3\,\text{GHz}$ and $d = \lambda_o/2$. (a) $f \geq f_o$, (b) $f \leq f_o$.

16.7% changes in the frequency result in 2.26°, and 1.67° respectively for the first null position.

3. SIMULATION RESULTS

To evaluate the performance of the proposed array, some computer simulations have been carried out in an ideal scenario without frequency fluctuation and in more realistic situations with frequency fluctuation. In the following, a uniform linear array with 10 elements and half-wavelength element spacing is assumed. The power of the desired signal is set to 10 dB, with respect to some reference level, and the power of the interference is set to 30 dB. The direction of arrival (DOA) of the desired signal is 0°, and the DOA of the interfering signal is 40°. For comparison purposes, the patterns of the original uniform array and the standard fully adaptive array are also illustrated. In the first test example, the result of applying the cancellation pattern due to the two edge elements only is illustrated. Here a region of wide (or sector) null extending from 60° to 90° is selected. The resulting pattern is shown in Fig. 2 together with the pattern of the original uniform array and that of the two edge elements. It is noticed that, the cancellation pattern due to the edge elements have forced a deep and wide null.

In the next example, the proposed array with two edge elements is to be compared with the traditional fully adaptive nulling array. The result is shown in Fig. 3. To achieve the deep null, the fully adaptive array shows higher sidelobes on both sides of the main beam as well as larger beam width as compared to the proposed array. More important, the proposed array exhibits a much wider null centered at 40°
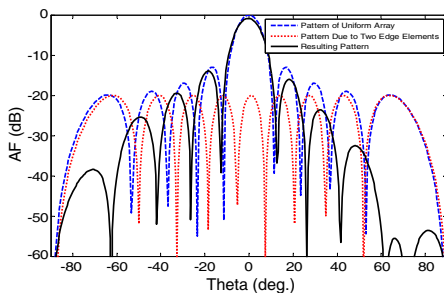
Figure 2. The cancellation pattern due to two edge elements (dotted red line) superimposed on the original uniform array pattern (dashed blue line), and resulting pattern (solid black line) when a sector null is placed between $60°$–$90°$.
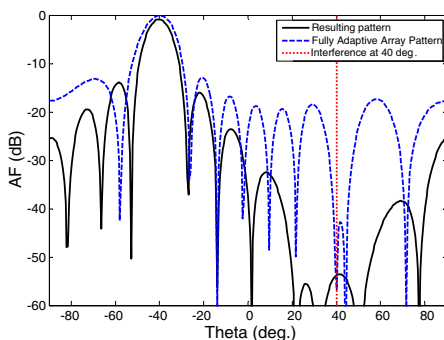

Figure 3. Placing a wide angular null centered at $40°$ in the pattern of the proposed array (solid black line), compared with that of fully adaptive nulling array (dashed blue line) for $N = 10$ elements, design frequency $f_o = 3$ GHz and $d = \lambda_o/2$.

Figure 4 shows the radiation patterns of the fully adaptive array, plotted at various frequencies. At the design frequency of 3 GHz, the null at the desired direction of $40°$ goes down to -100 dB. However, as frequency departs from the design value, the null moves away rapidly resulting in increased magnitude at the desired direction. It is noticed that the null is very sensitive to frequency changes.

Figure 5 shows the radiation patterns of the proposed array, plotted at various frequencies. The pattern maintains almost the same sidelobe level for the shown frequencies. At the design frequency of 3 GHz, the null at the desired direction of $40°$ goes down to -53.8 dB. However, as frequency departs from the design value, the null moves away slowly resulting in relatively increased pattern at the desired direction, but the magnitude of the pattern at the desired direction is
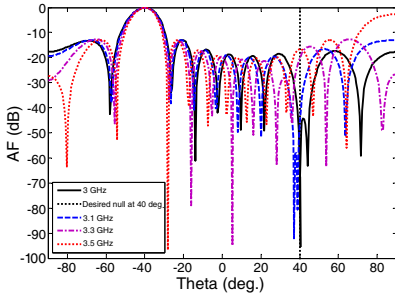
Figure 4. The effect of the frequency changes on the null positions in fully adaptive array for $N = 10$ elements, design frequency $f_o = 3\,\text{GHz}$ and $d = \lambda_o/2$.
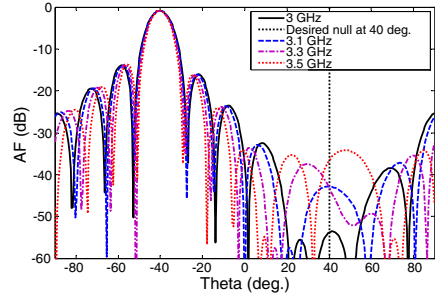
Figure 5. The effect of the frequency changes on the null positions in the proposed array for $N = 10$ elements, design frequency $f_o = 3\,\text{GHz}$ and $d = \lambda_o/2$.
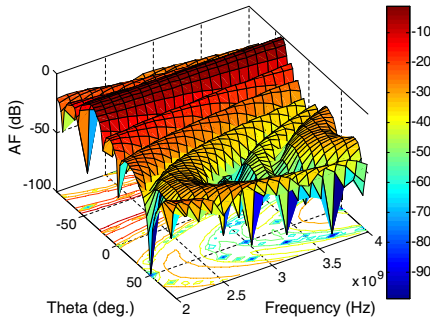

Figure 6. A 3-D plot of the pattern of the proposed array with a wide null centered at $40°$ and main beam scanned to $-40°$.
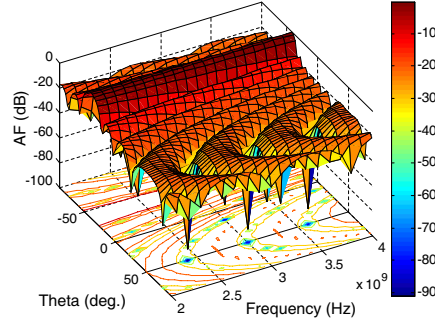
Figure 7. A 3-D plot of the original uniform array pattern with a main beam scanned to $-40°$.

still lower than $-36.6\,\text{dB}$ even at $3.5\,\text{GHz}$. It is noticed that the null of the proposed array has much lower sensitivity to frequency changes as compared to that of the fully adaptive array.

Figure 6 shows 3-D display of the resulting patterns at frequency range of interest. The displayed pattern is calculated using MATLAB subroutine *surfc*. Here, the main beam is steered to $-40°$ from broadside and the required wide null is centered at $40°$ as before (i.e., same as Fig. 5). As anticipated, the resulting null extends over large frequency range between 2.5–$3.5\,\text{GHz}$. At this band of frequency, the

null toward and around the desired direction goes down to $-50\,\mathrm{dB}$. For comparison purposes the original pattern of the uniform array has been plotted in Fig. 7 for the same frequency span. It is evident that the uniform array pattern exhibits deeper and much narrower null across the shown frequency band. Moreover the pattern shows more sensitivity to frequency and goes up as the frequency departs from the design value.

Figure 8 shows the variation of the depth of the null as the frequency of operation is varied between $2\,\mathrm{GHz}$ and $4\,\mathrm{GHz}$, for the array having design frequency of $3\,\mathrm{GHz}$. It can be seen from the figure that, the fully adaptive array has sharp and very deep null that can go down to $-100\,\mathrm{dB}$, while the null of the proposed array is wider and has minimum value of $-53.8\,\mathrm{dB}$ at the design frequency of $3\,\mathrm{GHz}$. The sensitivity to frequency can be seen from the slope of the figure around the design frequency of $3\,\mathrm{GHz}$. It can be easily noticed that the proposed array exhibits much lower sensitivity. From practical point of view, reducing the null depth to lower than about $-60\,\mathrm{dB}$ or $-70\,\mathrm{dB}$, will not be that effective as this level is near to the noise floor of the receiving system. However, when it comes to bandwidth, the proposed array can maintain acceptable null for much wider bandwidth. Assuming a value of $-40\,\mathrm{dB}$ as an upper limit for the acceptable null depth, then the fully adaptive array shows bandwidth of $0.25\,\mathrm{GHz}$, while the proposed array has much wider bandwidth of $0.9\,\mathrm{GHz}$, as can be seen from Fig. 8.

The next investigation is the performance of the array under signal and interference environment. Fig. 9 shows the calculated SINR at the
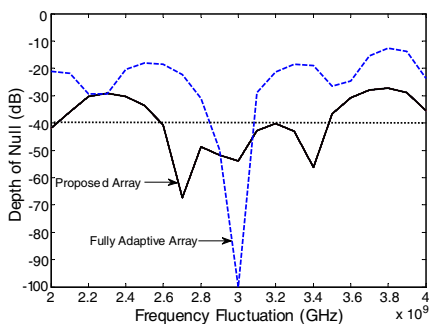

Figure 8. The depth of the null versus frequency changes over the S-band range.
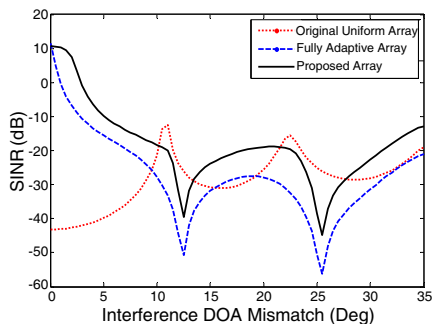

Figure 9. Performances of the tested arrays for $N = 10$ elements, design frequency $f_o = 3\,\mathrm{GHz}$ and $d = \lambda_o/2$ and various DOA mismatches.

design frequency of 3 GHz, for the case of one desired signal and one interfering signal impinging into the array from 0° and 40° respectively. The response is plotted against the mismatch (or departure) of the DOA of the interference source from the set direction of 40°. Here in this figure, the 0° angle, at the horizontal axis, is representing the case of no-mismatch (i.e., the assumed and true DOA are perfectly matched). For no-mismatch both arrays have almost the same SINR ratios of about 10 dB, which outperform that of the uniform array by 50 dB. However, as the DOA of the interfering source departs away, the performance degrades sharply especially for the fully adaptive array. A 5° departure can results in 20.5 dB reduction in the SINR for the proposed array, and 27 dB degradation for the fully adaptive array. The performance of the proposed array is better by at least a 6.5 dB over the shown range of angle mismatch. It can also be seen that the performance of the proposed array is better than that of the fully adaptive array all over the shown range of angle departure.

4. CONCLUSIONS

In conventional adaptive nulling arrays the nulls are very sensitive to frequency changes. Thus in most practical applications, the generated nulls should be deep and wide enough to accommodate frequency fluctuations. In this paper, an innovative technique for generating wide nulls to overcome the undesirable effects of frequency fluctuation has been presented. From the simulation results, it is noticed that the proposed array can maintain acceptable null for much wider bandwidth. Other advantages are that the pattern of the two edge elements has a small magnitude (less than -1 dB) at the main beam direction so that the gain is not much affected by the wide null formation. Moreover, the proposed array is much simpler than the fully adaptive array because it involves readjusting the excitation coefficients of the two edge elements alone whereas the interior elements keep their uniform excitation. The method can be easily extended to generate multiple wide nulls at prescribed directions by selecting other than two edge elements configuration for forming cancellation pattern.

REFERENCES

1. Applebaum, S. P., "Adaptive arrays," *IEEE Trans. on Antennas and Propagat.*, Vol. 24, 585–598, Sep. 1976.
2. Steyskal, H., R. A. Shore, and R. L. Haupt, "Methods for null control and their effects on the radiation pattern," *IEEE Trans. on Antennas and Propagat.*, Vol. 34, 404–409, 1986.

3. Lu, Y. and B. K. Yeo, "Adaptive wide null steering for digital beam forming array with the complex coded genetic algorithm," *IEEE Int. Conf. on Phased Array Systems and Technology*, 557–560, Dana Point CA, USA, 2000.

4. Haupt, R. L., "Phase-only adaptive nulling with a genetic algorithm," *IEEE Trans. on Antennas and Propagat.*, Vol. 45, No. 6, 1009–1015, 1997.

5. Li, W.-T., X.-W. Shi, L. Xu, and Y.-Q. Hei, "Improved GA and PSO culled hybrid algorithm for antenna array pattern synthesis," *Progress In Electromagnetics Research*, Vol. 80, 461–476, 2008.

6. Morabito, A. F. and P. Rocca, "Optimal synthesis of sum and difference patterns with arbitrary sidelobes subject to common excitations constraints," *IEEE Antennas and Wireless Propagation Letters*, Vol. 10, 623–626, Jul. 2010.

7. Mangoud, M. A.-A. and H. M. Elragal, "Antenna array pattern synthesis and wide null control using enhanced particle swarm optimization," *Progress In Electromagnetics Research B*, Vol. 17, 1–14, 2009.

8. Mouhamadou, M., P. Vaudon, and M. Rammal, "Smart antenna array patterns synthesis: Null steering and multi-user beamforming by phase control," *Progress In Electromagnetics Research*, Vol. 60, 95–106, 2006.

9. Mohammed, J. R., "Phased array antenna with ultra-low sidelobes," *Electronics Letters*, Vol. 49, No. 17, 18–19, 2013.

10. Compton, R. T., *Adaptive Antennas: Concepts and Performance*, Prentice-Hall, Philadelphia, PA, 1987.

11. Monzingo, R. A., R. L. Haupt, and T. W. Miller, *Introduction to Adaptive Arrays*, 2nd Edition, SciTech Publishing, 2011.

12. Van Veen, B. D. and K. M. Buckley, "Beam forming: A versatile approach to spatial filtering," *IEEE ASSP Mag.*, Vol. 5, No. 2, 4–24, Apr. 1988.

13. Morgan, D., "Partially adaptive array techniques," *IEEE Trans. on Antennas and Propagat.*, Vol. 26, No. 6, 823–833, 1978.

14. Haupt, R. L., "Adaptive nulling with weight constraints," *Progress In Electromagnetics Research B*, Vol. 26, 23–38, 2010.

15. Mohammed, J. R. and K. H. Sayidmarie, "A new technique for obtaining wide-angular nulling in the sum and difference patterns of monopulse antenna," *IEEE Antennas and Wireless Propagation Letters*, Vol. 11, 1242–1245, 2012.

16. Balanis, C. A. (edit.), *Modern Antenna Handbook*, John Wiley, 2008.